

Numerical Prediction of a Bangladesh Tropical Cyclone

T. N. KRISHNAMURTI¹, DARLENE OOSTERHOF¹ and DUSADEE SUKAWAT¹

(Manuscript received 25 November 1993, in final form 20 May 1994)

ABSTRACT

This paper deals with high resolution numerical weather prediction experiments for the recent Bangladesh Tropical Cyclone (April 1991). This devastating storm resulted in well over 100,000 deaths. The results from global model experiments carried out at a horizontal resolution of 213 waves (triangular truncation) and from a regional model at a horizontal resolution of 46 km are presented. Recent improvements in the model's parameterization of cumulus convection, land surface parameterization (the specification of ground wetness), enhanced evaporation over low wind speed regions were included in the sensitivity studies reviewed here. The improvements to the model results were also contributed by two data sets, one a high resolution sea surface temperature over the Arabian Sea and the other a satellite based surface wind estimate from microwave radiometer. These appear to provide strong positive impact during the storm's landfall history. Overall we demonstrate the results of successful landfall experiments with the high resolution global and regional models where we have incorporated the aforementioned improvements, i.e. in the data sets and in the physical parameterizations.

(Key words: Global modelling of tropical cyclone)

1. INTRODUCTON

A salient feature over the Bay of Bengal is the annual north south migration of the ITCZ. (A list of acronyms appear in Table 1) The convergence zones's passage near 10°N is a critical element especially around April, May and October, November, i.e. the pre and the post monsoon respectively. During these months the ITCZ is generally located over a region of warm sea surface temperatures of the order of 29°C and the tropospheric vertical wind shear is a minimum near that region. These appear to be important factors in the formation of tropical cyclones. Figure 1 illustrates the 850 mb climatological motion field based on 15 years of data covering 1960 to 1979. Here we illustrate the monthly mean flow vectors for the months April and November at 850 mb. The interesting and relevant feature is the

¹ Department of Meteorology, Florida State University, Tallahassee, FL 32306-3034, U.S.A.

Table 1. List of Acronyms.

DMS	D efense M eteorology S atellite P rogram
ECMWF	E uropean C entre for M edium- R ange F orecasts
GW	G round W etness
ITCZ	I nter-tropical C onvergence Z one
JMA	J apan M eteorological A gency
JTWC	J oint T yphoon W arning C enter, G uam
NMC	N ational M eteorological C enter
NOAA	N ational O ceanic and A tmospheric A dministration
SSM/I	S pecial S ensor M icrowave I mager
SST	S ea surface t emperature
UTC	U niversal t ime c oordinate

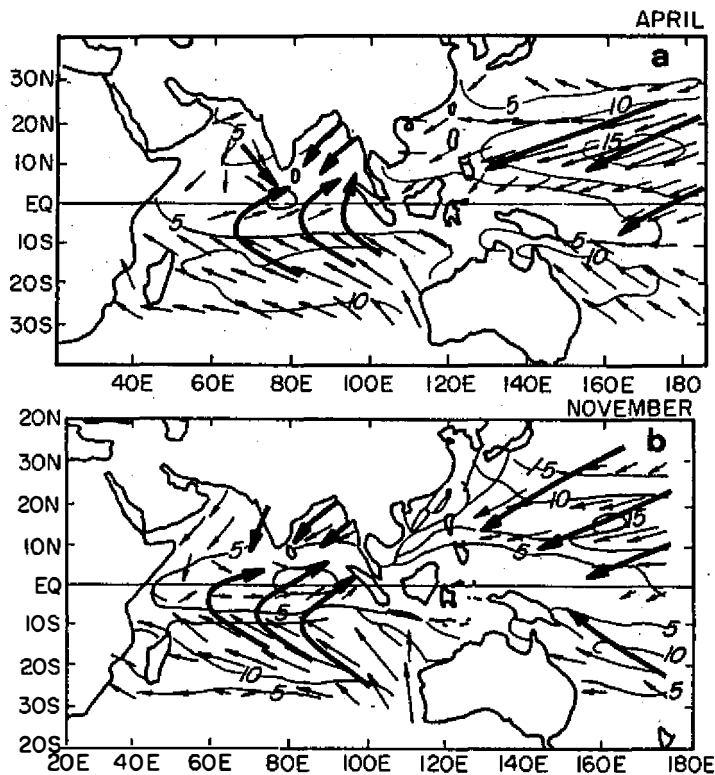


Fig. 1. 850 mb climatology based on 15 years of data 1960 to 1979. Top panel shows the flows for April and bottom panel shows the flows for November. Source: RAND Climatology from NCAR.

asymptote of convergence of the cyclonic wind. That line is located near 10°N in the months when the Bay of Bengal cyclogenesis is known to be prevalent. Satellite strip photographs of x-t charts, e.g. Wallace (1970), illustrate the passage of cloud clusters that move from the western Pacific Ocean westward into the Bay of Bengal. Some of these tropical waves are known to develop into tropical cyclones. An x-t diagram of the outgoing longwave radiation for the belt 5°N to 15°N illustrate this westward passage of a wave-like structure, Figure 2; this wave culminated in the formation of the major tropical cyclone of April 1991. In this illustration we show three heavy lines. One of these roughly along 80°E denotes a stationary cloud system; this was a long lasting cloud system over southern India along 10°N. It was present over this region for almost 10 days between the 20th and 30th of March 1991. A westward propagating cloud cluster meets this stationary cloud system around the 26th of March when heavy rains were noted over southeastern India. The Bangladesh cyclone was, in fact, associated with another westward propagating cloud cluster (heavy slanted line to the right). This system arrives near 90E around the 27th of March. This zonal time section along 10N does not show the time history of the storm beyond the 27th since the storm moves north of 10°N. The climatological fields of SST for the months of maximum frequency of cyclones (April and November) are shown in Figures 3 a and b. The region around 10°N over the Bay of Bengal experiences temperatures in excess of 28°C. This is one of the characteristic features of the cyclogenetic region. The ocean temperatures were slightly warmer in November as compared to April.

Examining the SST fields for the specific year April 1991, we noted that the SST anomalies for this month were in fact quite different from the climatology over the Bay of Bengal local warm ocean anomalies exceeding 2°C were noted over the western Bay during April 1991. Our modelling studies revealed a large sensitivity to these SST anomalies in

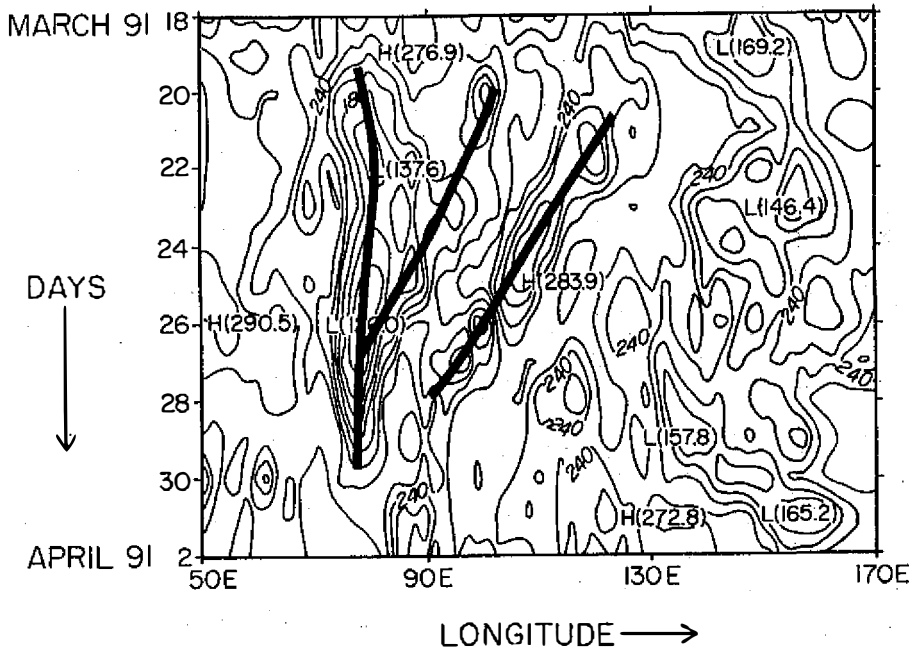


Fig. 2. Time longitude diagram of the outgoing longwave radiation (units watt m⁻²) from March 18 to April 2, 1991 illustrating the westward passage of a wave like disturbance carrying low OLR values.

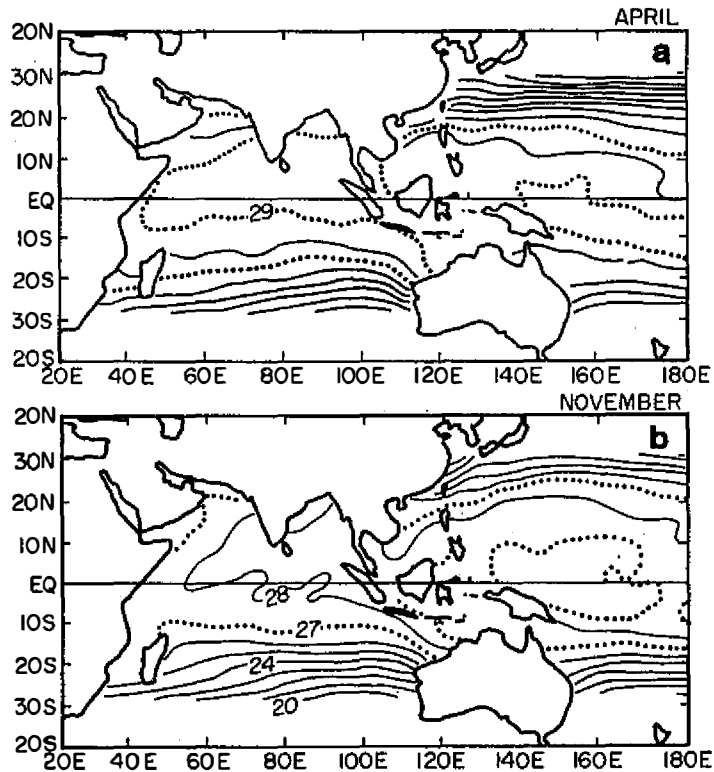


Fig. 3. Climatological sea surface temperatures for the months April and November. Interval of analysis 1°C, the 27 and 29° isopleths are dotted. Source: RAND Climatology from NCAR.

strengthening the tropical cyclone to super typhoon intensity. This SST field is illustrated later in this paper in section 7. That region of cyclogenesis is illustrated in Figure 4; here we have shown the tracks of all major storms of the last 10 years that made a landfall over Bangladesh. Of major interest is the region of the south-central Bay of Bengal where most cyclones form, this is roughly bounded by 87.5°E and 95°E and 8°N and 17.5°N. This region is usually under surveillance from satellite observations. We have highlighted the April 1991 storm by the heavy legends on the dates (at 00 UTC),

The frequency of storms that make landfall over Andhra Pradesh (eastern India) and over Bangladesh appear to show a slight preference to the El Niño years and the El Niño year minus one respectively. This appears to be an important climatological finding (Gupta and Muthuchami ; 1991). Figures 5 a and b illustrate these tracks for recent storm tracks for the El Niño year and the year 'El Niño minus one'. One can easily see a somewhat preferred channelling of storms towards Andhra Pradesh or Bangladesh during these respective years. The difference in the steering of storms, during these respective years, can be seen in the vertically integrated tropospheric flow fields. A westward phase shift of the subtropical high during the El Niño years provides a deeper tropospheric easterly flow on its southerly flank which helps storms to enter the east coast of India during the El Niño year. During the 'El Niño minus one' year the subtropical high is located farther eastward and a southerly

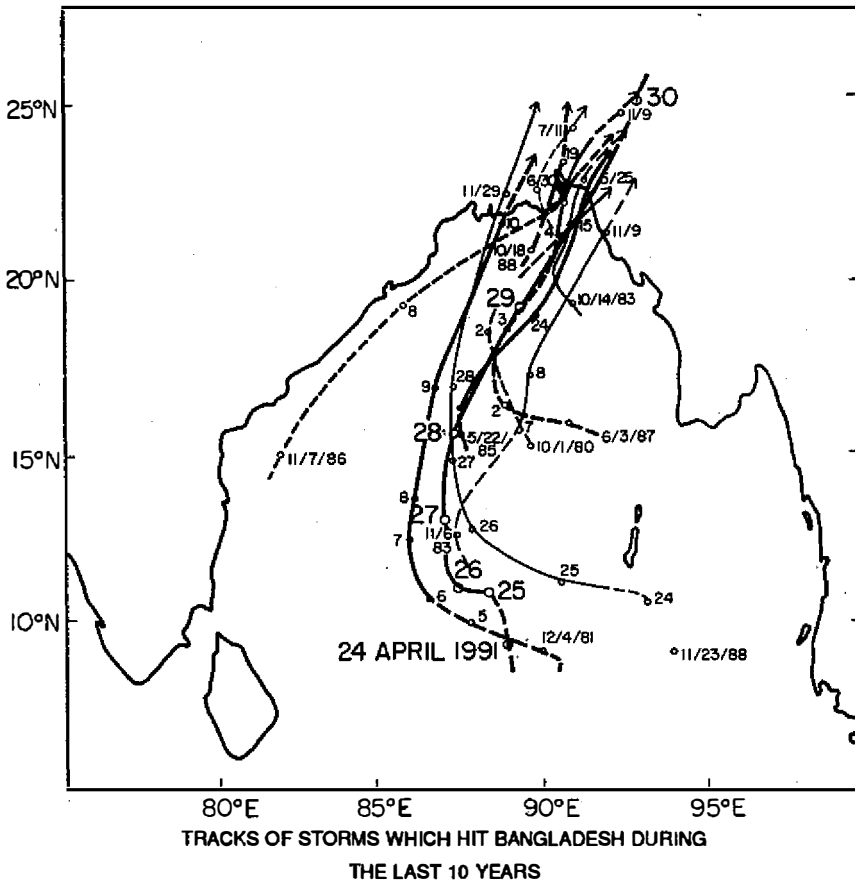


Fig. 4. Tracks of storms that made landfall over Bangladesh between 1981 and 1991.

steering of the vertically integrated flow helps the storms to move more northward over the Bay of Bengal. The west Pacific high appears to shift eastward from roughly 120°E to 100°E during the El Niño year. During the pre and post monsoon months, April and November, the middle latitude tropospheric westerly current extends south of the Himalayas. As a consequence, a rapid eastward steering of the Bay of Bengal cyclones is encountered as they approach 20°N . This is one of the factors that contributes to the recurvature of the storms towards Bangladesh.

Bangladesh storms have been known to cost the largest number of human lives. The recent storm of April 1991 produced strong winds and roughly 20 feet waves resulting in almost 118,000 deaths. The coastal region of Bangladesh along the Bay of Bengal is illustrated in Figure 6. Islands such as Hatia and Sandwip and low lying areas to the north along Majidi, and to the west along Bura, Guaranga and Bhola and to the east along the entire coastal stretch between Chittagong and Cox's Bazaar are all severely affected by storm passages. The April 1991 cyclone affected the coastal area of Chittagong with well

over 20 foot tides. The astronomical tidal history of this period is illustrated in Figure 7. This storm made its landfall over the Chittagong area on April 29th at around 22 UTC. That was close to the 30th at around 0400 local time. The tidal history shows a high tide of about 12 feet around this time. The storm tide added to that produced wave heights close to 20

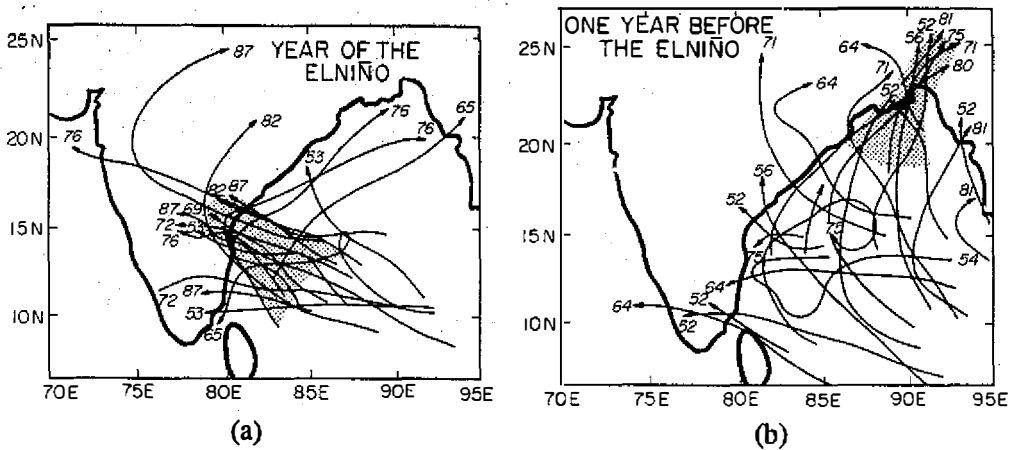


Fig. 5. Storm tracks during (a) El Niño years and (b) during a year prior to the El Niño.

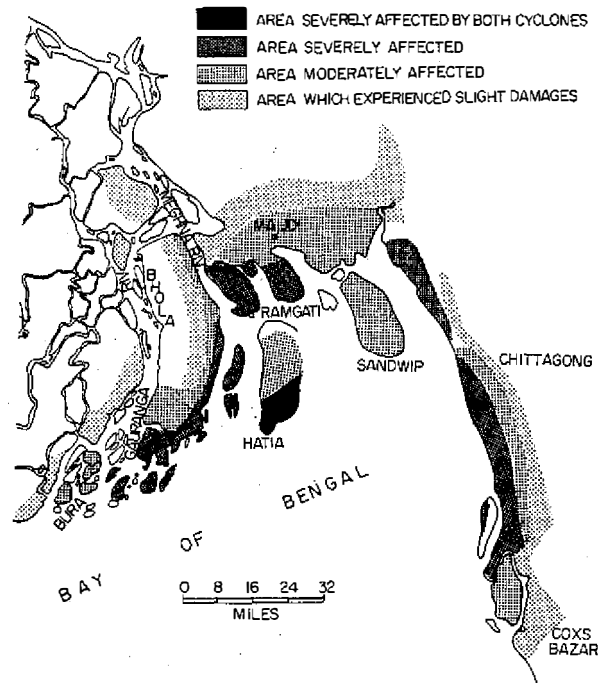


Fig. 6. The coastal regions of Bangladesh and the severity of typical storm damage.

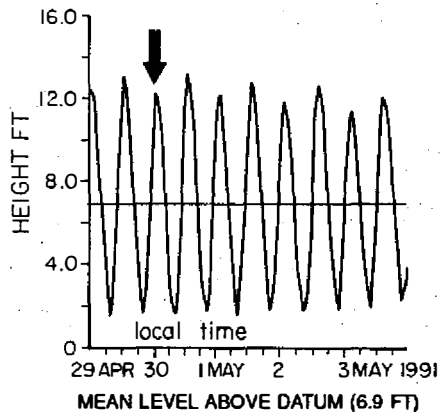


Fig. 7. Astronomical tide over Chittagong during 1991. The high tide around April 30 coincided with the period of landfall.

feet over the coastal area of Chittagong. According to eyewitness accounts, three such waves occurred over intervals of 4 to 5 minutes each causing most of the deaths in the low lying area of Chittagong. Concrete bunkers, over coastal areas, built on 20 foot stilts have saved the lives of several hundred people who witnessed the fury of the storm and came down from the bunkers, almost a day later, as the water subsided. Forecasts provided by JTWC in Guam were available almost 48 hours in advance via the U.S. Embassy in Dakka, however the evacuation of a million people from the Chittagong area of Dakka simply was not possible. Table 2 lists a history of some of the major storms of the Bay of Bengal covering the years 1737 to the present time. Estimated storm tides, estimated maximum winds and the reported loss of life are listed here. Among these, the most severe of the storms were the ones during 1737, 1876, 1970, and 1991. Since 1980 there have been 9 significant cyclones that affected Bangladesh. As will be seen from this study, atmospheric forecasts of these storms on the time scale of 2 to 3 days have improved considerably, but the handling of accurate storm surge forecasts is still quite premature; it is this aspect which deserves much further research because the loss of life is related to storm surges. The maximum storm tides of the earlier storms of the 18th and 19th century were reported to be as high as 40 feet. That perhaps, may be open to question, nevertheless the reported deaths in excess of 200,000 lives were based on best available official reports. The November 1970 storm was another of the very extreme category. That storm led to a closer cooperation in science between U.S. and Bangladesh resulting in the installation of a digital Radar (Frank 1971). Although atmospheric storm forecasts have improved dramatically, as may be seen from this study; the disaster is more directly a consequence of storm surge and practical difficulties of evacuation of people from low lying areas.

The history of the April 1991 storm based on the Guam summary is illustrated in Figure 8. This illustration provides the chronology of the tropical cyclone development starting from 25th of April 1991 when the mean winds were of tropical storm stage. The storm acquired maximum strength on April 29th at 12°E, when the wind speed reached 260 KPH (72 ms^{-1}). NOAA 11, the U.S. operational polar orbiting satellite, provided an IR imagery some 5 hours after the maximum intensity was reached. Figure 9 illustrates this imagery. A very well defined eye, eye wall and rain bands are evident in the illustration. One of the bands extends into India from the south of the storm.

Table 2. Some of the significant cyclones in the Bay of Bengal.

Date	Area affected	Maximum storm tide (ft)	Maximum wind (knot)	Estimated deaths
1737(Oct)	South of Calcutta	40		300,000
1789(Dec)	Coringa			30,000
1864(Oct)	Calcutta	40		80,000
1876(Oct)	Bakarganj	30-40		215,000
1885(Sep)	False Point	22		10,000
1926(May)	Burma			1,200
1941(Jun)	Barisal			5,000
1942(Oct)	Bengal	16	80-85	40,000
1949(Oct)	Southeastern India			1,000
1960(Oct)	Bangladesh	12	60	6,000
1960(Oct)	Bangladesh	20	113	4,000
1961(May)	Bangladesh	16	90	2,000
1963(May)	Bangladesh		130	22,000
1964(Dec)	Ceylon	15-20		1,800
1965(May)	Bangladesh	12	85	15,000
1965(Dec)	Bangladesh	12	120	15,000
1970(Nov)	Bangladesh	20	130	300,000
1971(Oct)	Orissa	20	100	10,000
1977(Nov)	Southeastern India	19	135	14,000
1979(May)	Southeastern India	13	85	700
1984(May)	Southeastern India	10	85	430
1985(May)	Bangladesh	15	60	11,000
1991(Apr)	Bangladesh	22	140	138,000

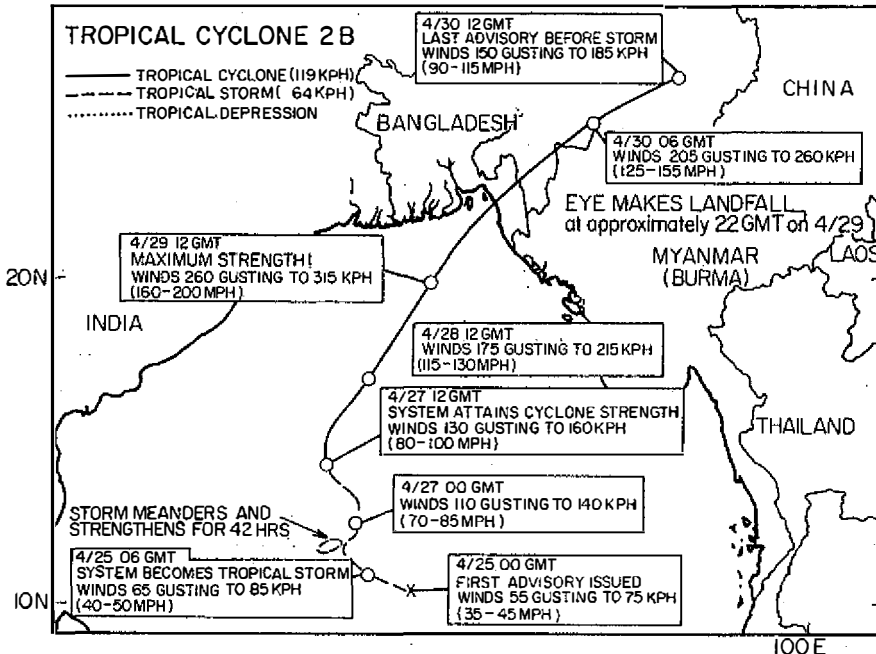


Fig. 8. Chronology of the storm intensity between April 25 0000 UTC 1991

2. OBSERVED MOTION FIELD AT 850 mb

The operational analysis from both the NMC and the ECMWF were available to us. Lacking adequate data and bogussing of storms over the Bay of Bengal, the models had mislocated the center of circulation; our efforts to use these analyses for verification of forecasts would thus be only qualitative over the ocean. Figures 10 illustrates the NMC analysis at 850 mb for hours 0, 24 and 48 of our forecast period. In this analysis large position errors, in the location of the storm, were apparent at hours 0, 24 and 48 hours. The more relevant feature in these analysis is the northerly circulation over India which is evidently a response to the lowering of pressure over the Bay of Bengal. A strong component of this northerly flow exits the Indian land mass near 16°N over the Bay of Bengal coast and moves over the warm sea surface temperature anomaly. The air-sea interaction of these surface flows result in a strong moisture flux from the ocean to atmosphere which is in turn

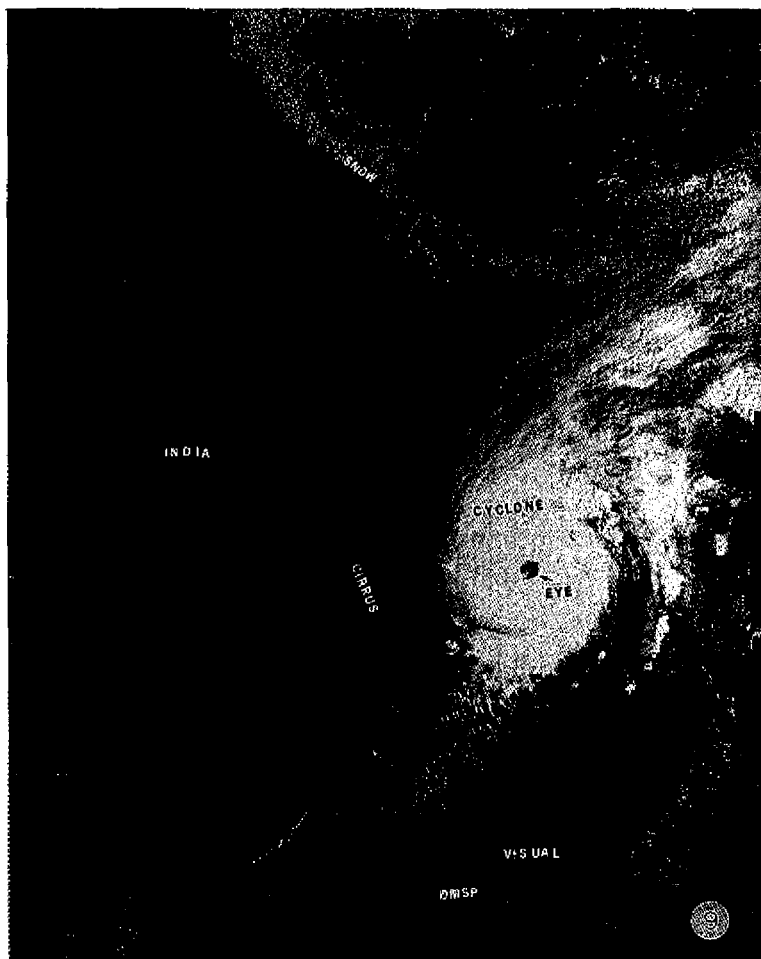


Fig. 9. A visual satellite imagery of the Bangladesh storm on April 29 1000 UTC, 1991. This is just prior to the landfall. The storm center can be located from the information presented in Figure 8.

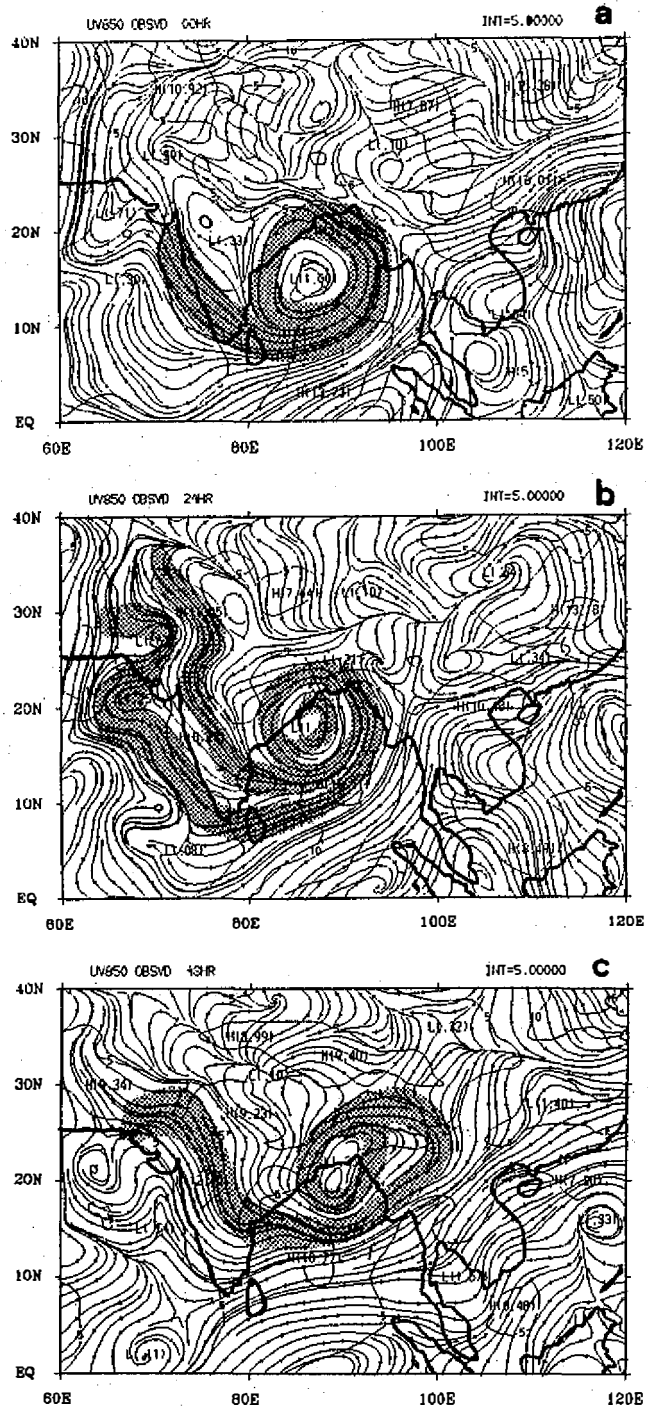


Fig. 10. Operational NMC analysis at 850 mb for: Top: April 28, 1991 00Z (t=0); Middle: April 29, 1991 00Z (t=24 hours); Bottom: April 30, 1991 00Z (t=48 hours)

supplied to the storm circulation. The response of the circulation over India to the storm over the Bay of Bengal and the air-sea interaction are important aspects of this storm's history.

3. DESCRIPTION OF THE MODELS

Table 3 provides an outline of the two high resolution models that were used for the prediction of the Bangladesh cyclone. The model described on the left half of this table is a global spectral model and the one described on the right half is a high resolution regional model. Very briefly these "respectively" may be described as i) a global spectral transform model at a horizontal resolution T213 and 15 vertical levels and ii) a semi-implicit semi-Lagrangian model at a horizontal resolution of 0.46° latitude/longitude and 15 vertical levels. Both models include fairly comprehensive physical parameterization and initialization algorithms. They, in addition, include orography consistent with the resolution of the respective models.

It is of interest to note that the predicted heavy rainfall area during 33 to 36 hours of forecast (April 29, 0900 UTC to 1200 UTC) does correspond very closely to the location of the typhoon as seen in Figure 9.

Table 3. Regional and Global Forecast Models.

Parameters	Regional Model Krishnamurti et al. (1990)	Global Model
Independent Variables	Longitude, latitude, sigma (vertical coordinate), time	Longitude, latitude, sigma (vertical coordinate), time
Dependent Variables	zonal wind U, meridional wind V, vertical velocity σ , pseudo pressure function P, specific humidity q, surface pressures p_s , geopotential ϕ	streamfunction ψ ; velocity potential X, vertical velocity σ , pseudo pressure function p, pseudo vertical velocity w, dew point depression S, surface pressure p_s , geopotential ϕ
Horizontal Advection	Semi-Lagrangian	Spectral transform method Machenhauer (1972), Pasch (1983)
Vertical Advection	Finite difference	Finite difference
Time Differencing	Semi-implicit	Semi-implicit
Resolution Horizontal	46 km	Triangular truncation T213
Resolution Vertical	15 levels	15 levels
Orography	Envelope at model resolution	Envelope at model resolution Wallace (1983)
Physical processes	Surface similarity fluxes	Surface similarity fluxes Businger (1971)
	Disposition of fluxes in vertical (mixing length)	Disposition of fluxes in vertical (mixing length) Tiedke (1984)
	Dry convective adjustment	Dry convective adjustment Kanamitsu (1975)
	Modified Kuo Deep Convection	Modified Kuo Deep Convection Krishnamurti et al. (1983)

4. THE PREDICTED MOTION FIELD

It was felt that the time history of the predicted motion field at 850 mb would be most revealing of the quality of the Bangladesh tropical cyclone forecast. The experiment we describe here is the T213 version of the global model described in the left portion of Table 3. Figure 11 illustrates the predicted motion fields at intervals of every 6 hours starting from hour 6 of the forecast. The heavy solid numbers denote the maximum wind speed of the storm at 850 mb which changes sequentially as 28, 43, 31, 51, 53, 49, 41 and 28 ms^{-1} during the forecast from hour 6 to hour 48 at 6 hour intervals. The model at T213 does not attain the proper supertyphoon strength at hours 24 through 36 but does reach a maximum intensity close to 50 ms^{-1} . Overall the prediction of the intensity and track are quite impressive. The central portion of the storm is handled extremely well through the landfall. Another striking feature of this forecast is the swath of northerly flow that develops over India in response to the intensification of the storm over the Bay of Bengal. That feature was noted in the

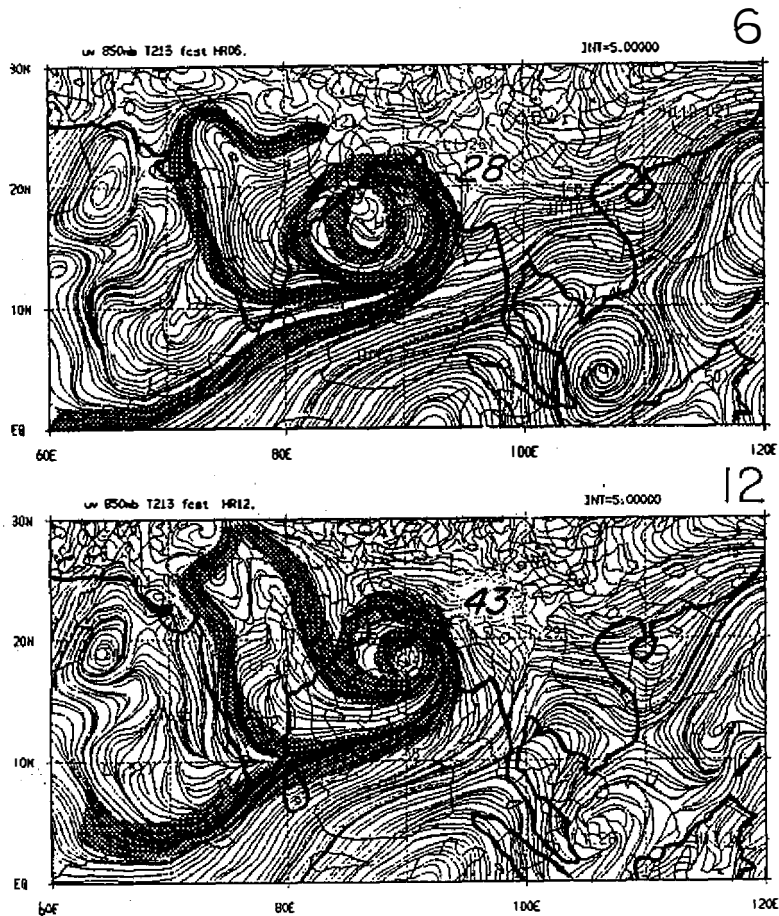


Fig. 11. Predicted 850 flow field between hour 6 to hour 48. The maximum wind speed (ms^{-1}) of the storm is entered in dark numbers next to the Bangladesh storm.

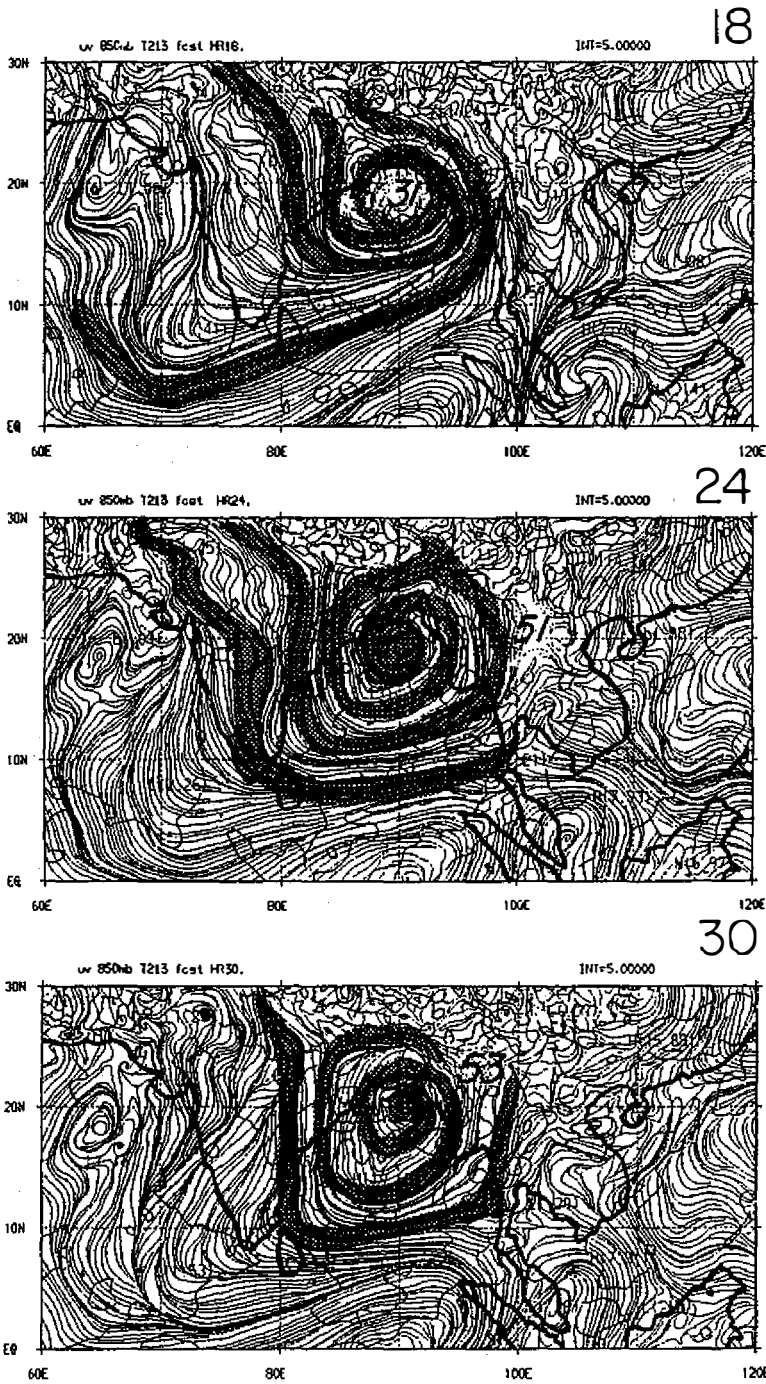


Fig. 11. (Continued.)

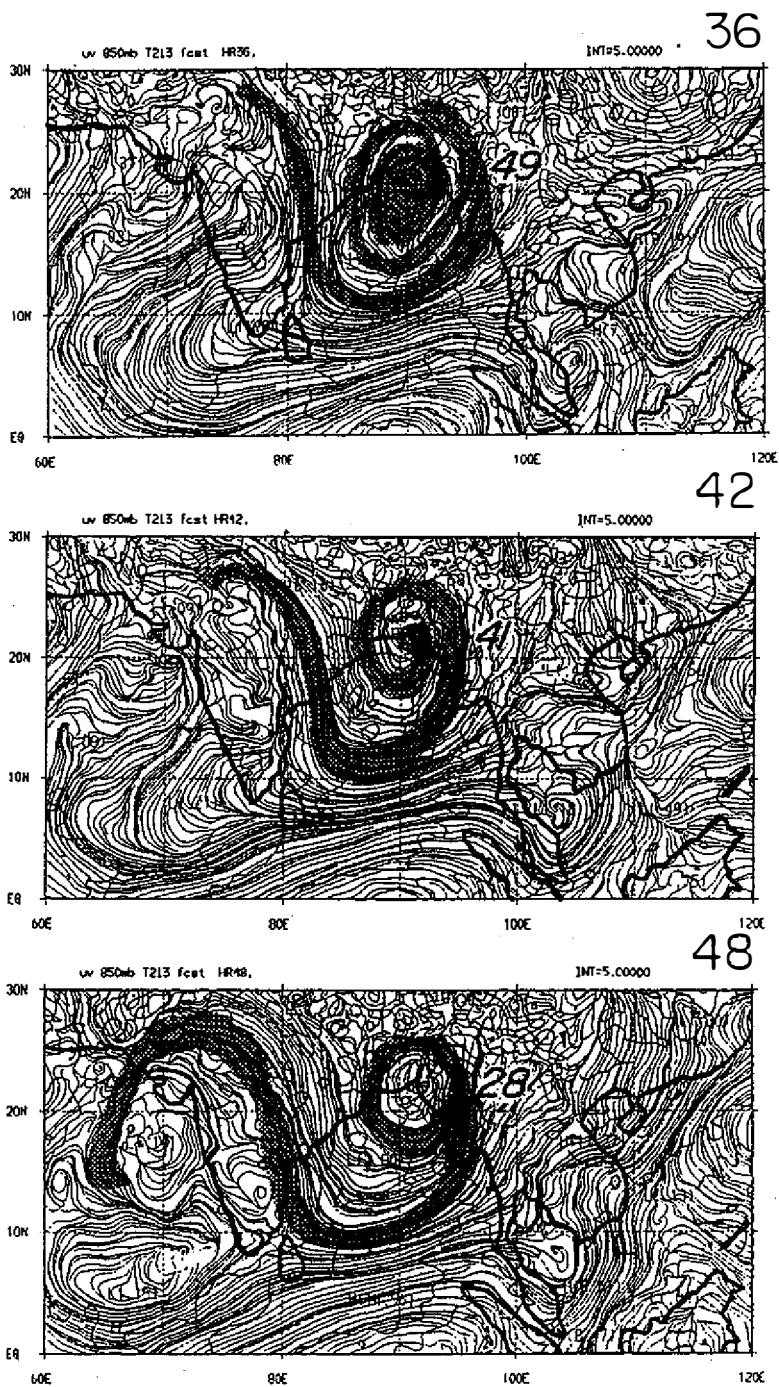


Fig. 11. (Continued.)

observations. The presence of the supertyphoon over the Bay of Bengal results in pressure changes as far as central India. Other features such as the strengthening of the southwest monsoon flows south of India enhances the rainfall over the Indochina region which was also handled reasonably well by the global model.

Some of the salient aspects of the global forecast at the resolution T213 are summarized in Figure 12. The top left panel shows a comparison of the observed and the predicted storm track for the 42 hour forecast. The 6 hourly precipitation at landfall is shown in the top right panel which indicates rainfall rates of the order 150 mm/day over the Chittagong area. The evolution of the eye like characteristics are clearly evident in θ_e cross sections by hour 36 of the forecast. The left panel shows the initial configuration of θ_e . These vertical-zonal cross-sections were applied through the center of the storm. The bottom two panels show the 850 mb circulations leading to the landfall. Here the strongest winds during landfall are evident over the Chittagong area. This was based on the complete version of the model described in the right half of Table 3.

5. PRECIPITATION FORECASTS

Figure 13 illustrates the time history of the predicted 3 hourly rainfall from the global model run at the resolution T213. Rainfall rates of the order of 16 mm/day were noted in the first 3 hours. A rapid growth of the rainfall is noted in the forecast. The organization of rainfall is best evident after 15 hours when the tropical cyclone intensity is reached. Rainfall amounts continue to increase and reach magnitudes of around 280 mm/day after hour 24 of the forecast. Just prior to landfall, between hours 33 and 36, rainfall rates exceed an intensity 400 mm/day. The color panel Figure 12 illustrates the rainfall pattern between 36 and 42 hours as the tropical cyclone was making a landfall. During this 6 hour period the rainfall rates had reduced to roughly 150 mm/day.

6. EQUIVALENT POTENTIAL TEMPERATURES

In the numerical simulation of hurricanes with a global model we had noted that the steady maintenance of realistic θ_e structures near the region of the eye wall requires a steady generation of moist static instability in the storm environment (Krishnamurti *et al.*, 1992). The role of radiative processes in the undisturbed storm environment appeared to be critical for medium range prediction. The shallow stratocumulus clouds of the storm environment provided a steady stream of radiatively destabilized inflowing air in the sub cloud layer. The minimum values of θ_e were found to be maintained by the cloud top cooling. A detailed cloud-radiative algorithm was required to model the maintenance of the inner rain area of the hurricane. The same band model of long wave radiation based on the work of Harshvardhan (1984) and cloud specification based on threshold relative humidity (Krishnamurti *et al.*, 1990), was used in the present study. At the resolution T213 we were able to generate narrow near constant θ_e profiles along the vertical near the storm axis, Figure 14. During hours 12 through 30 of forecast, the θ_e profiles exhibit a minimum value along the vertical at around 600 to 700 mb for the storm environment. The eye of the storm, however, is characterized by a near constant θ_e along the vertical. Initially, a minimum value prevailed near 600 to 700 mb everywhere as the tropical cyclone was intensifying; at 48 hours the eye had started to weaken as the storm began to draw continental air into its circulation in its northwestern flank.

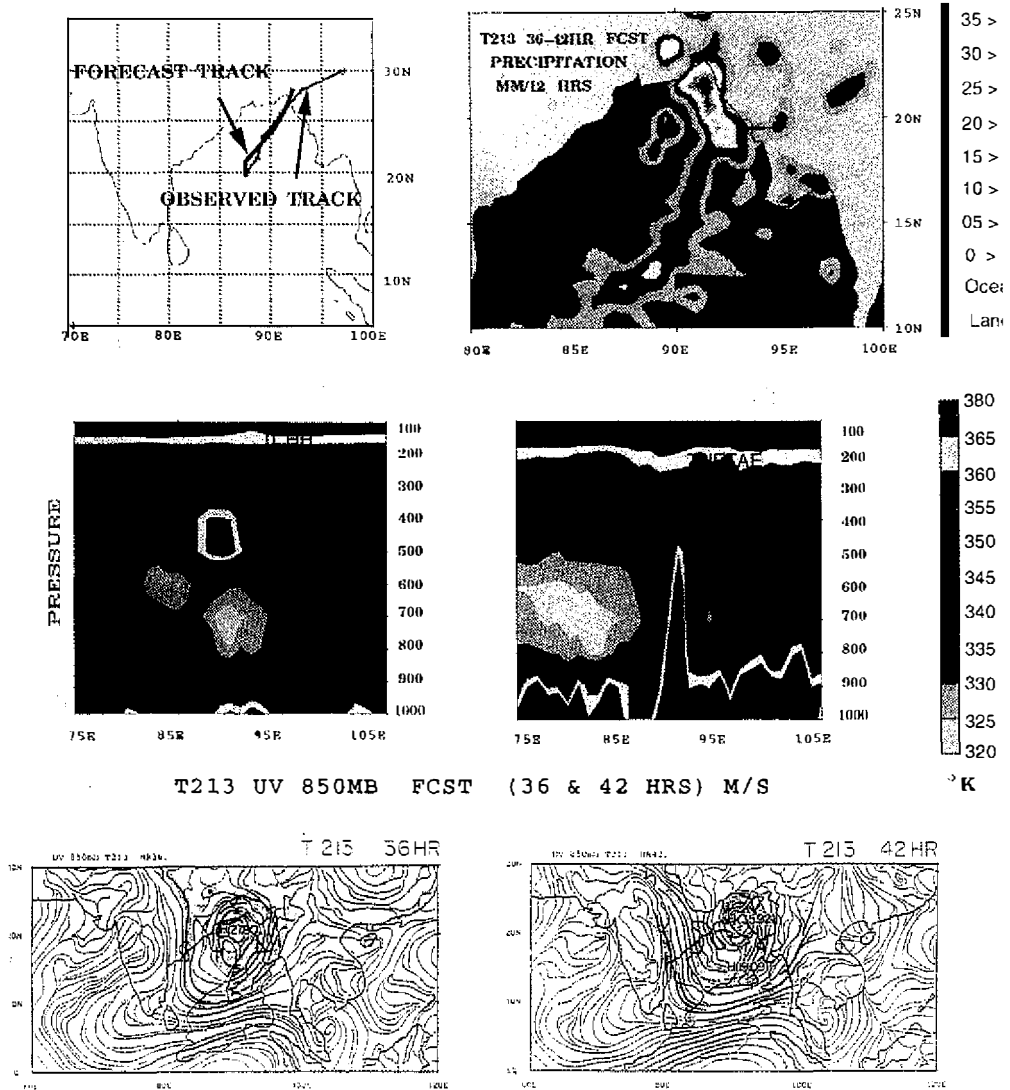


Fig. 12. A summary of the global model (T213 resolution) results around the land-fall period. Top left: Observed and predicted tracks. Top right: 12 hour accumulated rainfall at the landfall. Middle left: θ_e pressure-longitude cross section across the prestorm depression at hour 0. Middle right: θ_e pressure-longitude cross section across the tropical cyclone at hour 36. Bottom left: 850 mb streamlines at hour 36 of forecast. Shaded area has wind speed greater than 20 ms^{-1} . Bottom right: 850 mb streamlines at hour 42 of forecast. This is close to the period of landfall. The shaded area has wind speed greater than 20 ms^{-1} .

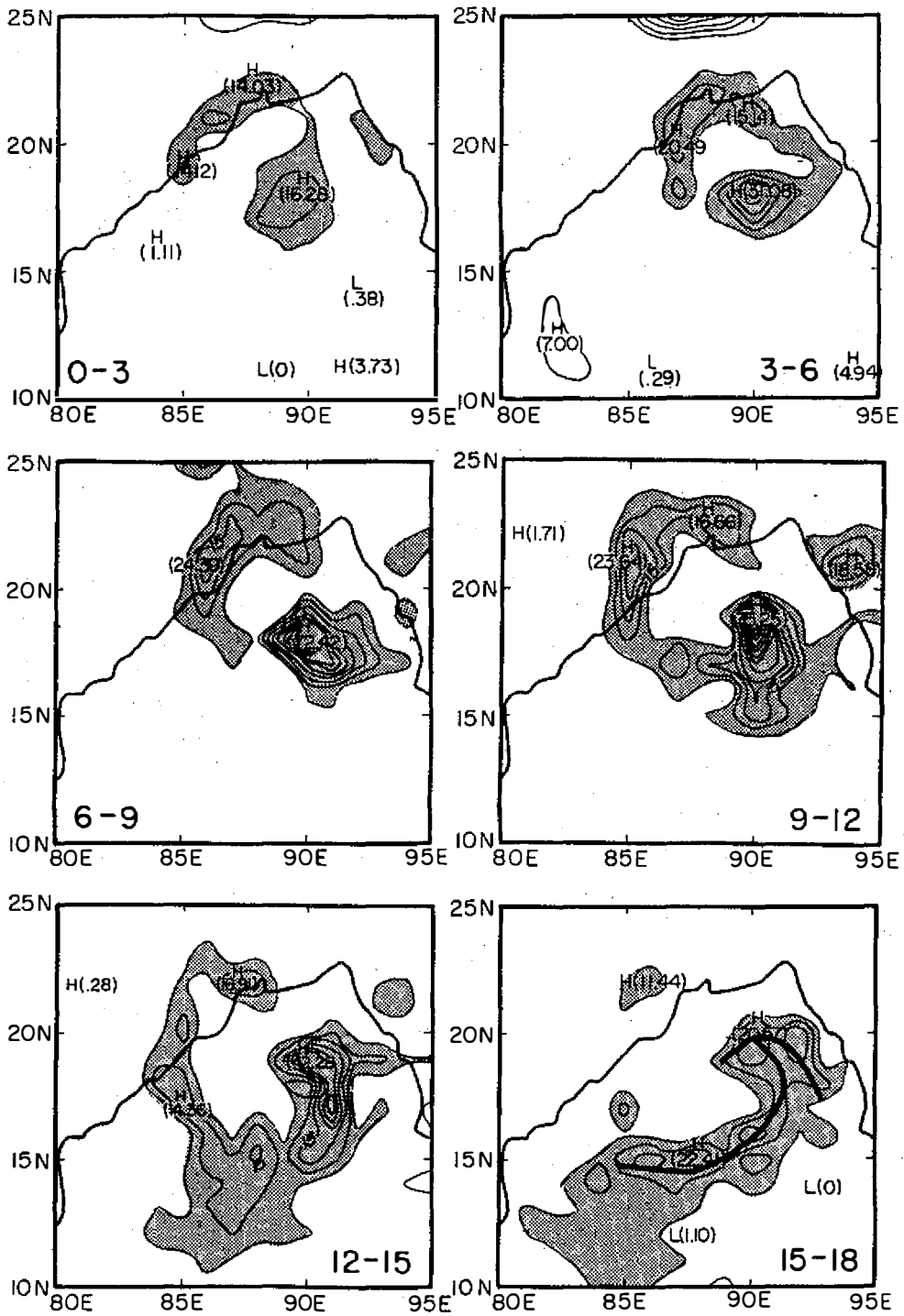


Fig. 13. Predicted rainfall (T213 resolution) every three hours from hours 0-3 through hours 45-48. Units mm/3 hours. Shaded area greater than 5 mm/3 hours.

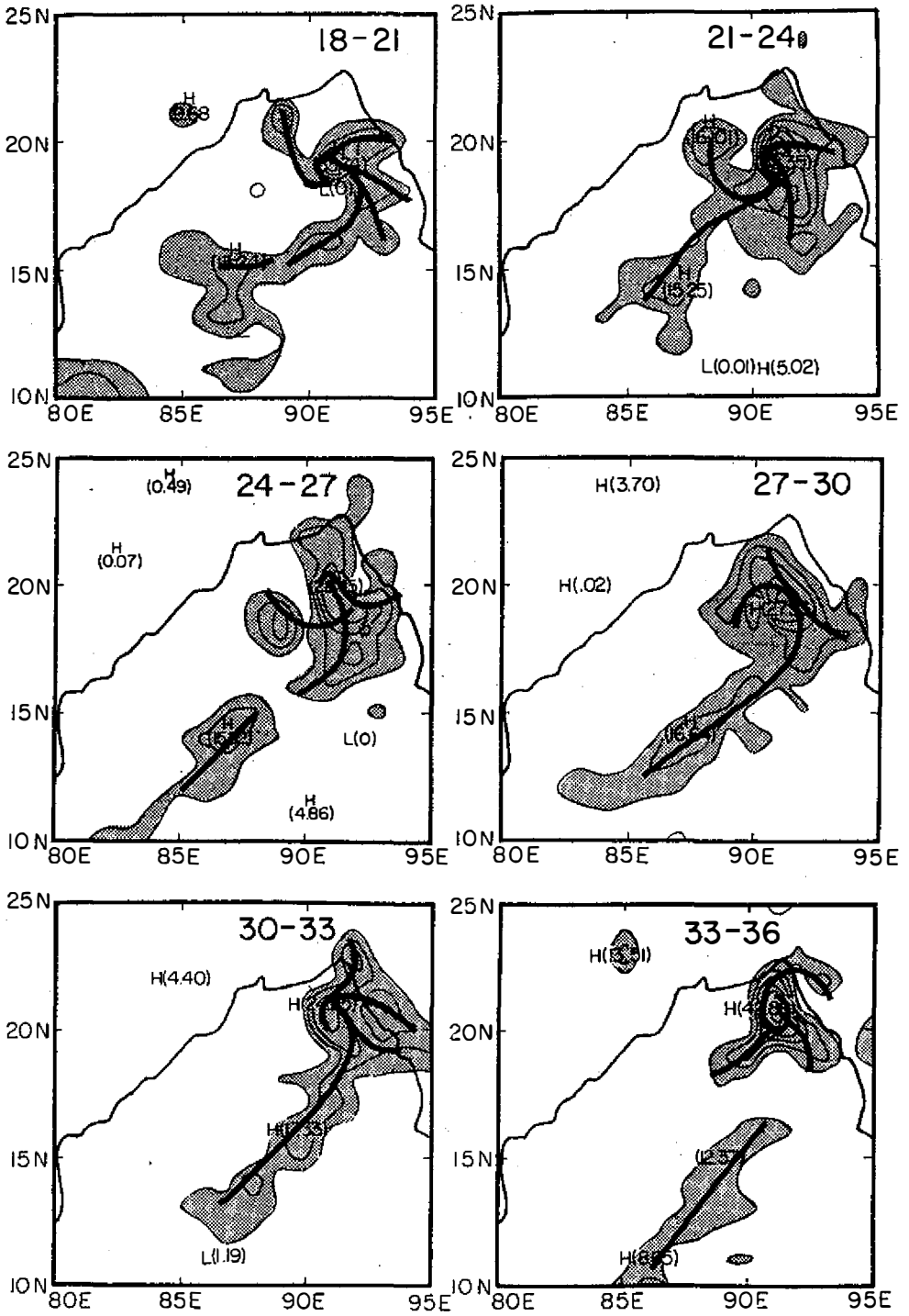


Fig. 13. (Continued.)

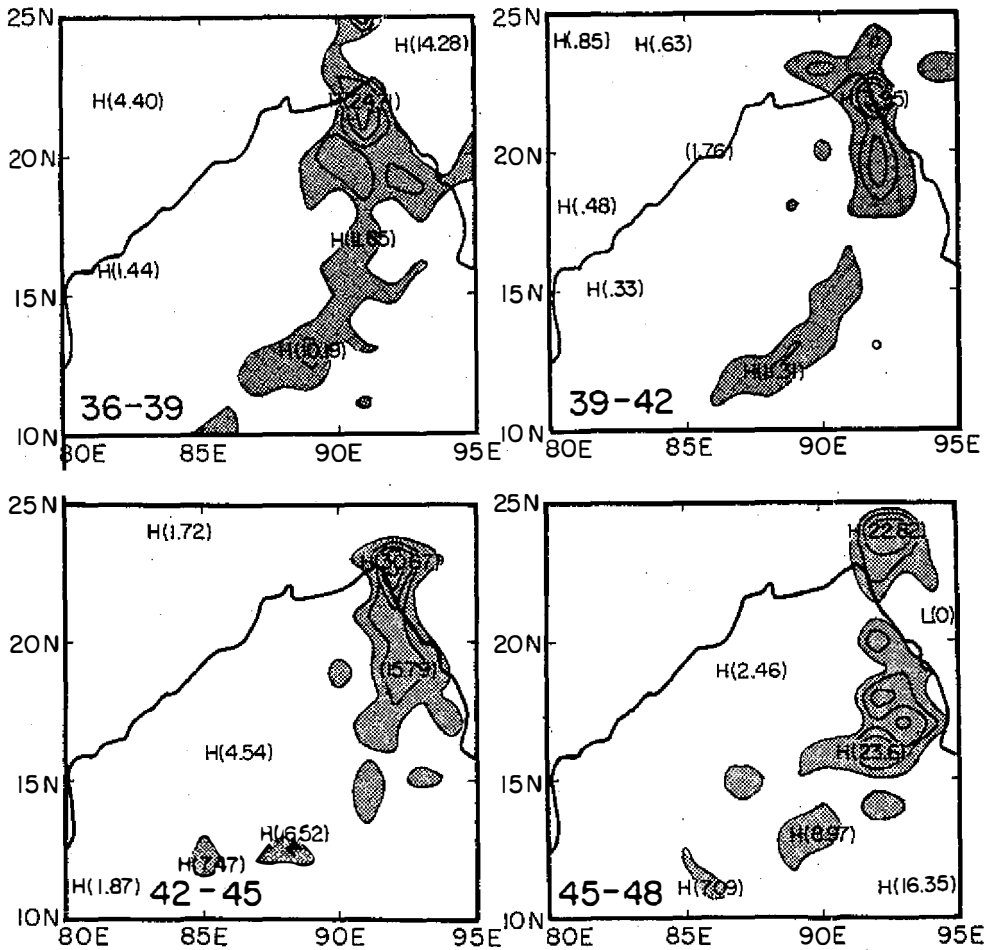


Fig. 13. (Continued.)

7. SENSITIVITY EXPERIMENTS

Most of the following sensitivity experiments are based on a study by Sukawat (1992). This work was done using a multilevel regional model at a horizontal resolution of 46 km, and 15 vertical levels (See the left half of Table 3).

7.1 Sea Surface Temperatures

The storm track appeared to be most sensitive to the specification of sea surface temperatures. Two versions of sea surface temperature data were available for a 10 day period covering the dates April 21 through April 30, 1991. One of these was the operational SST analysis of the NMC and the other was the operational product from JMA. The latter contained a warm SST anomaly which is illustrated in the center left panel of Figure 19. This will be discussed later. The SST value over this region was just over 30°C. This was located somewhat to the west of the cyclone track. The observed flow field, see Figure 10, from India was entering the storm circulation passing over this warm ocean. The surface flows exhibit

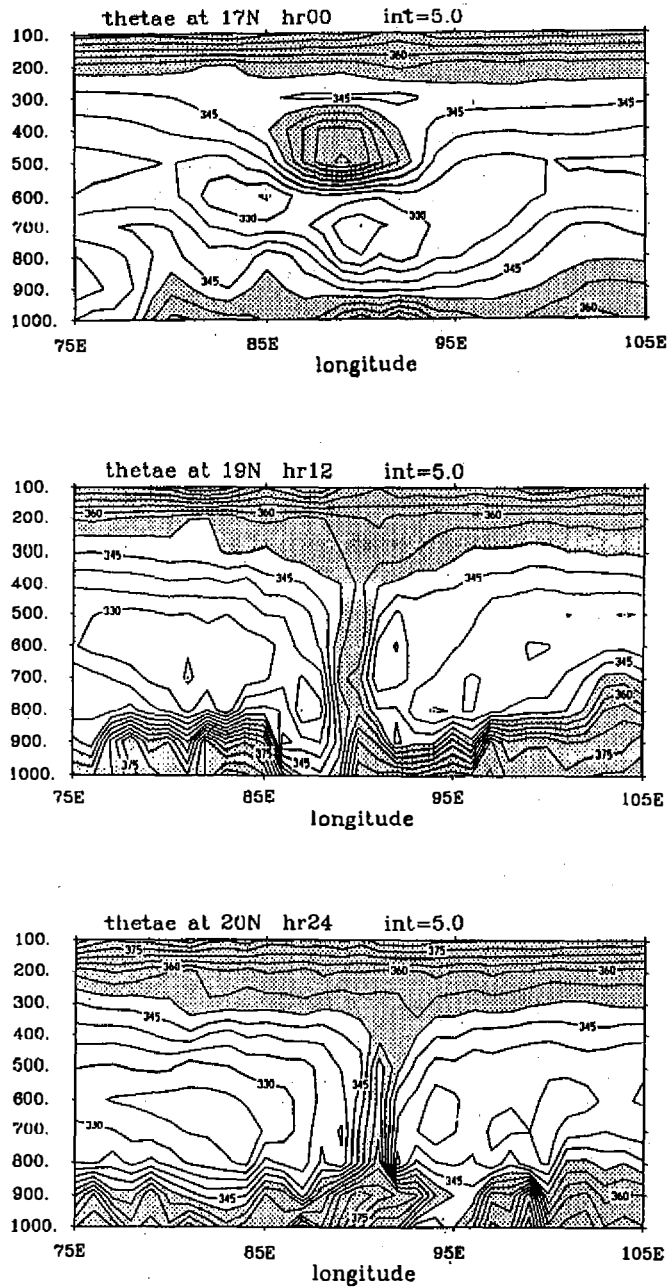


Fig. 14. Predicted vertical-zonal cross section of the equivalent potential temperature θ_e between hours 0 and 48 and 12 hourly intervals. A vertical tube of near constant θ_e (along vertical) denotes the establishment of the warm core and the modelled eye wall. At hour 48 this feature starts to get eroded as landfall occurs.

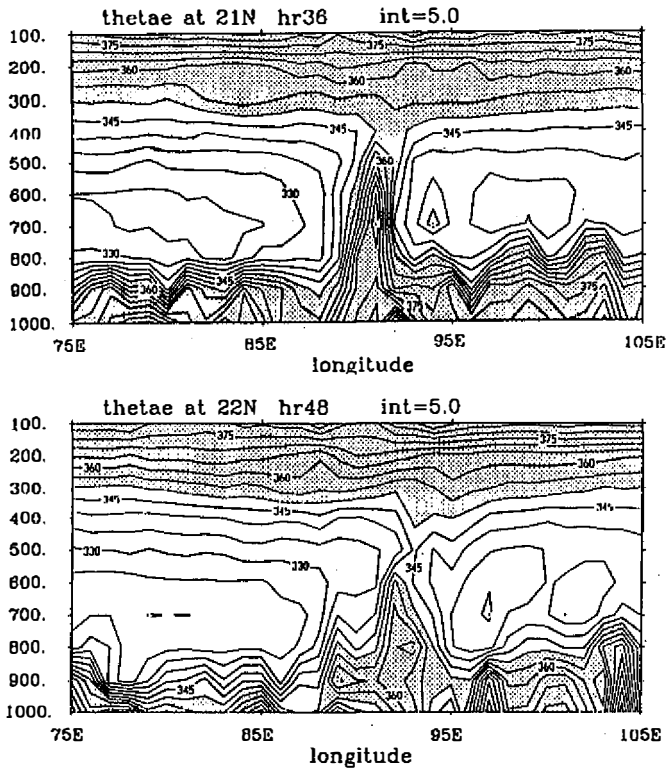


Fig. 14 (Continued.)

larger air sea interaction, i.e. larger flux of latent heat from the ocean to the atmosphere, where this warmer SST anomaly is used in the forecast experiment. The surface moisture flux on day 3 of forecast (April 30, 00 UTC) are illustrated in Figure 15. The top panel of this diagram shows the results for a control experiment where the NMC's operational sea surface temperatures were used, these did not include a warm SST anomaly over the western Bay of Bengal. The bottom panel describes the fluxes (on day 3 of forecast) for the second set of SST's that were obtained from the Japan Meteorological agency. This was based on a special collection of marine data and describes the warm sea surface anomaly over the Western Bay. Overall, we note a marked difference in the fluxes over the warm pool (see Figure 15) and in the vicinity of the storm. The fluxes were weaker over the storm regions for the control case since the storm was less intense. In the experiment with the warm SST anomaly we noted much larger fluxes in the vicinity of the warm anomaly and in the storm region. Thus it appears to support our conjecture that the swath of offshore flow from India coming in contact with the warm SST anomaly undergoes stronger air-sea fluxes of moisture which gets transmitted to the storm laterally and perhaps that is a factor for the more intense storm when compared to the control case.

7.2 Land Surface Parameterization

In a recent study Dastoor and Krishnamurti (1990) noted a marked sensitivity of tracks of landfalling storms to the ground wetness parameterization. Basically a past rainfall spell during a premonsoon dry season close to the track of a landfalling hurricane appeared to

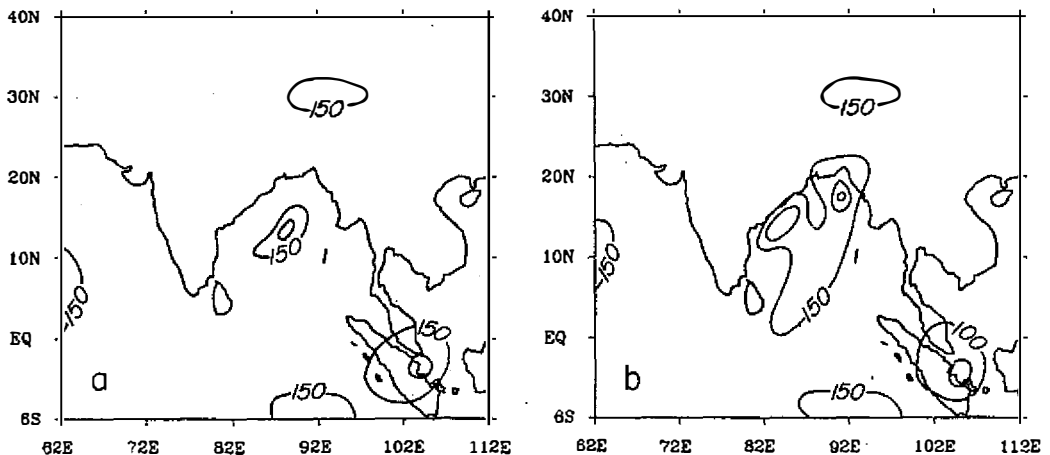


Fig. 15. Top: Surface fluxes for day 3 of forecast (watts m^{-2}) for a control experiment that was based on NMC's SST field.
 Bottom: Surface fluxes for day 3 of forecast (watts m^{-2}) for an SST anomaly experiment where we used the SST from the Japan Meteorological Agency.

influence the storm track. That behavior was also noted for the Bangladesh cyclone of April 1991 (Sukawat; 1992). In this study two versions of ground wetness (GW) parameterization were tested; one a classical method (where the GW was simply a function of surface relative humidity and surface albedo) was compared to a surface energy based land surface model where the GW was a function of past rainfall, ground temperature, surface humidity, elevation and surface albedo. For details of these methods reference may be made to Dastoor and Krishnamurti (1990). Figures 16a, b, c and 17a, b, c illustrate the time evolution of the ground wetness for these two respective formulations. It should be noted that the improved ground wetness does not only depend on past rainfall, factors such as surface humidity, ground temperature and albedo. As a consequence these two overall fields are quite different. A swath of ground wetness extends along the storm track for the experiment where the ground wetness parameterization includes the past rainfall. The classical method describes a ground wetness evolution over India and the use of this method resulted in larger track forecast errors. These results on the Bangladesh storms were somewhat analogous to our computations for the landfall of a tropical cyclone over southeastern India during the first week of May 1979, Dastoor and Krishnamurti (1990). In that study we had noted a strong influence of pre-storm rain in providing a swath of large ground wetness along which the storm eventually moved.

7.3 Enhanced Evaporation

Two versions of surface similarity fluxes were compared. One of these uses a standard formulation of surface similarity theory following Louis (1981) and Krishnamurti *et al.* (1988). The other version involves a parameterization of vertical eddy flux of momentum in low wind speed regions following Beljaars and Miller (1990). The storm environment contains several regions of low wind speed, where the wind speed is less than 5 ms^{-1} . Contrary to our intuition this increased evaporation had a negative impact on the intensity of the storm. When the evaporation was enhanced over the immediate storm environment, the

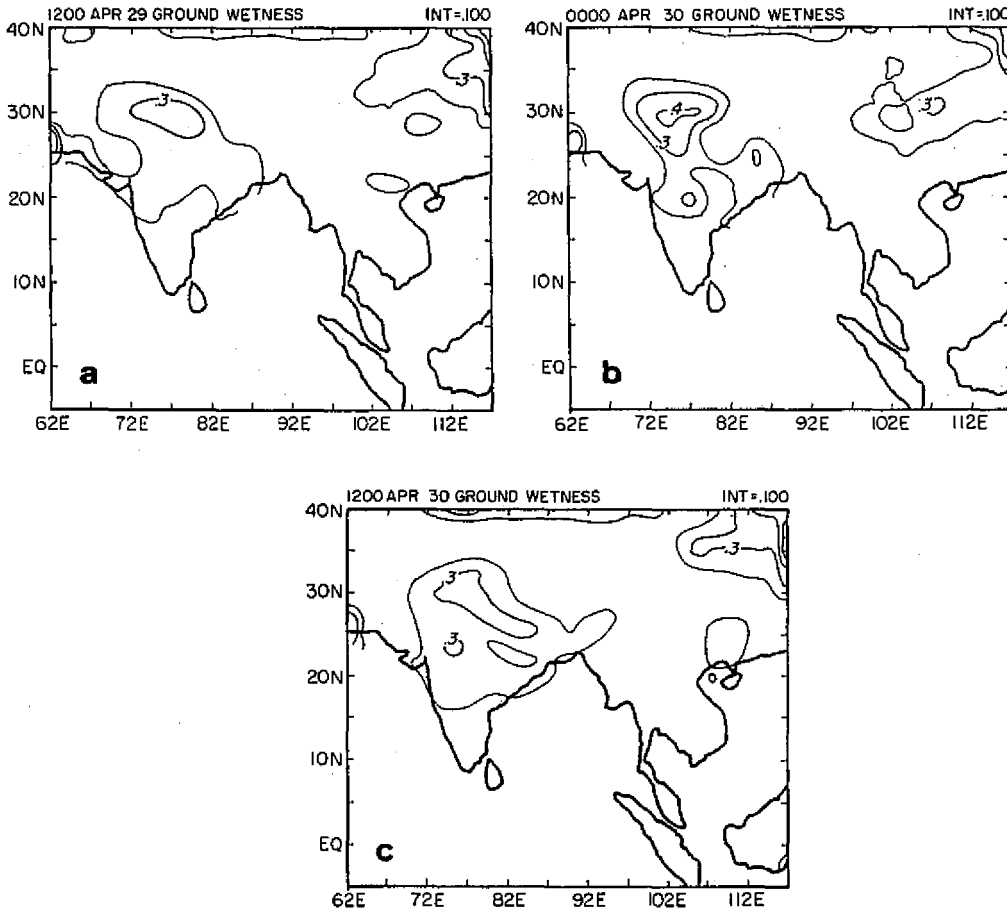


Fig. 16. Distribution of ground wetness parameter based on a simple parameterization, i.e. function of surface albedo and surface relative humidity. Forecast fields for a) April 29 12 UTC, b) April 30 00 UTC and c) April 30 12 UTC are shown here.

inflowing surface air brought moist air next to the ocean in the high wind speed area. In this region the difference between the saturation relative humidity at the ocean temperature and that of the surface area is in fact reduced; as a result evaporation was reduced in the storm area. This resulted in a 10% reduction in the storm intensity. The regions of the warm SST anomaly over the Western Bay was not affected by the enhancement of surface fluxes since the surface wind speeds over that region for both experiments were in excess of 5 ms^{-1} .

7.4 The Burmese Mountains

An artificial reduction of the Burmese Mountains by as much as a kilometer was introduced to assess the effect of the Burmese Mountains on the passage of the Bangladesh cyclone. The geometry of the mountains: the normal mountain, the reduced mountain and their differences are illustrated in Figures 18a, b and c. The effects of reduction of the

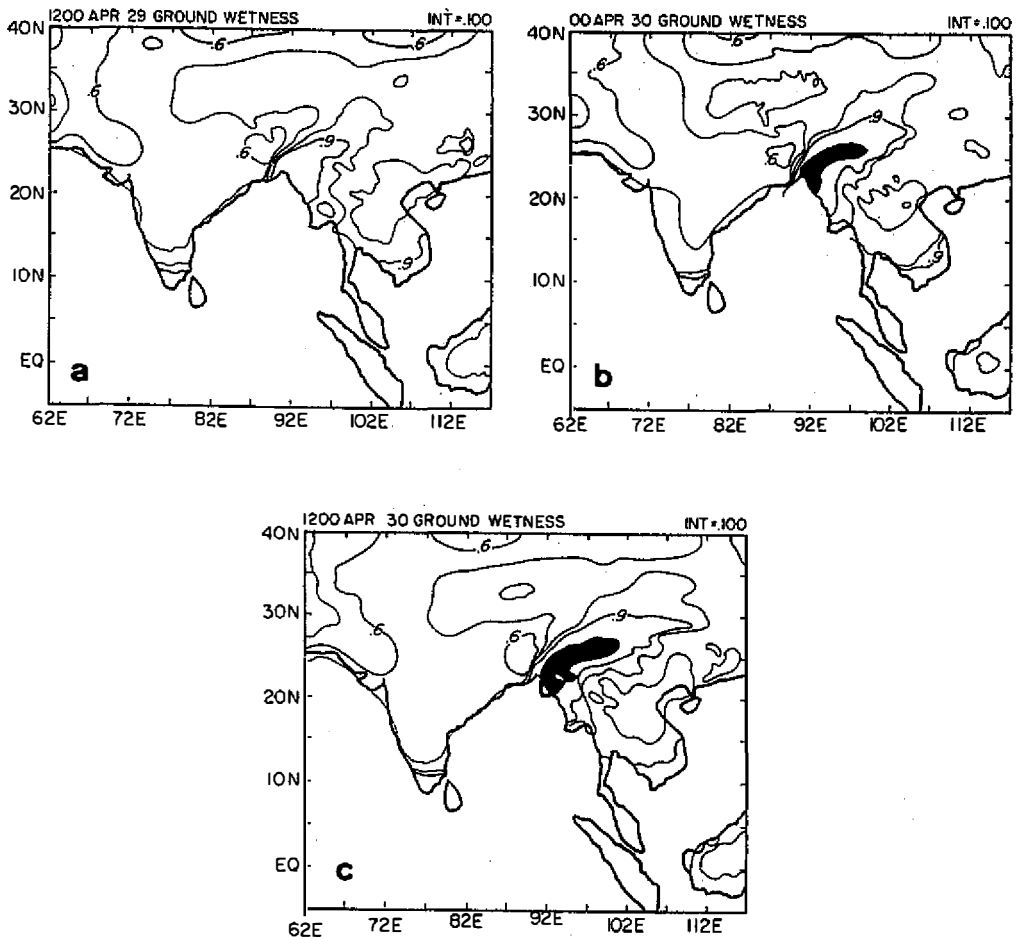


Fig. 17. Same as Figure 16 but for a ground wetness parameterization that includes past rainfall and several other parameters.

Burmese mountains are illustrated in Figures 18d and e. The track of the storm for the reduced mountain deviated slightly to the left compared to that for the steeper mountain. Perhaps the most conspicuous difference in these two experiments was in the lower tropospheric wind speed after landfall. The 60 hour forecast showed almost 7 ms^{-1} stronger surface winds for the reduced mountain experiment. The reduced mountain also resulted in a reduction of rainfall amounts. Between hours 24 and 60, the effects of orography were largest for the storm rainfall, during this period the reduced mountain experienced a reduction of rainfall by as much as 30 mm/36 hours.

7.5 Inclusion of Surface Winds from the Satellite Microwave Data

The Defense Meteorology Satellite Program (DMSP) launched several satellites with microwave radiometers in recent years. Besides providing useful data for rain rate estimates this data set has also been used to provide estimates of surface wind speeds. The Special

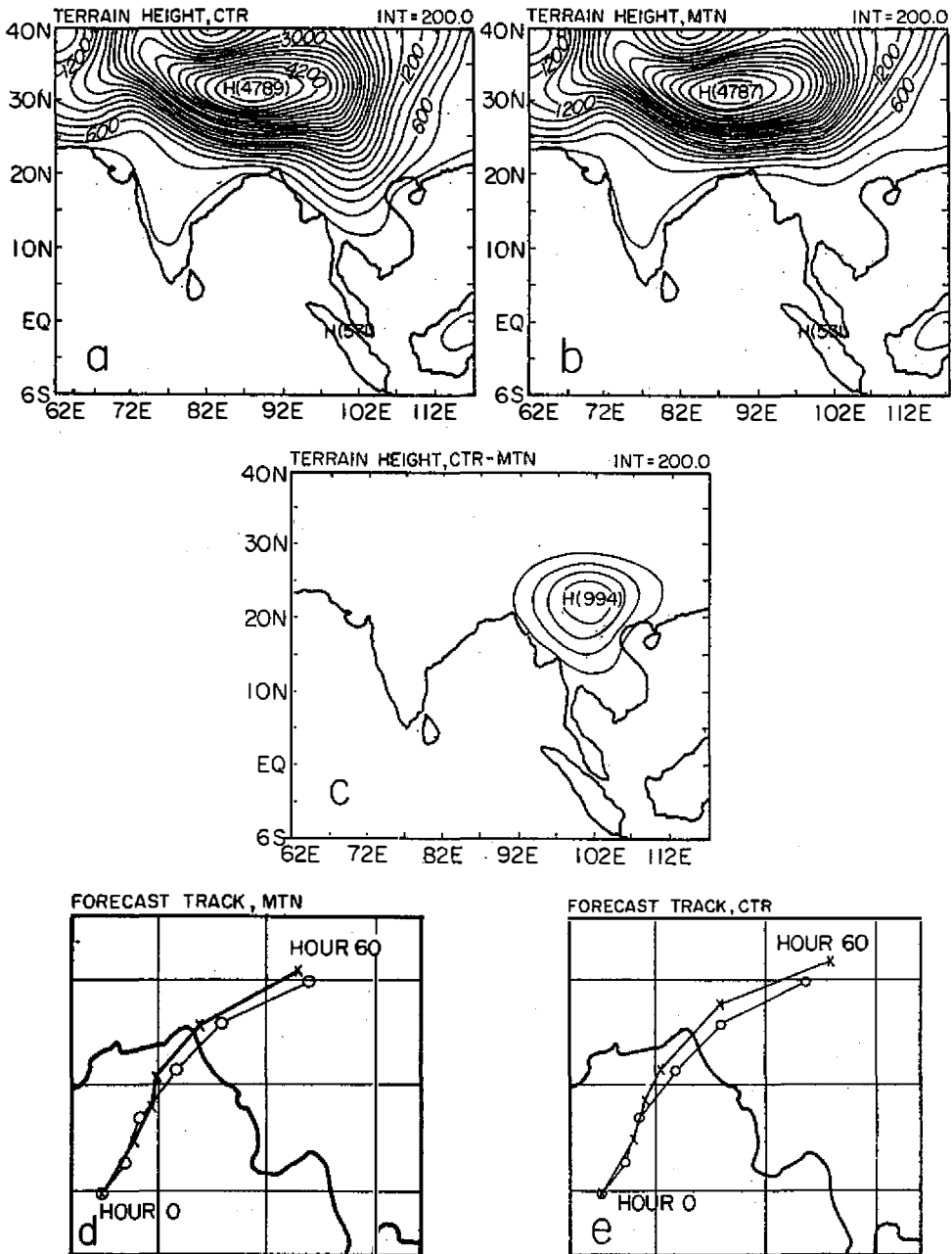


Fig. 18. (a) Normal terrain elevation used in the regional model forecast experiment, units: meters. (b) Terrain heights where the Burmese Mountains were artificially suppressed, units: meters. (c) Difference of panel 'a' minus panel 'b', units: meters. (d) Track chart for the normal terrain experiment. Open circles: observed track; Closed circles: predicted track. (e) Track chart for the terrain experiment where the Burmese Mountains were artificially excluded. Open circle: observed track; Closed circle: predicted track.

Sensor Microwave Imager (SSMI) contains 4 frequencies. It receives both vertical and horizontal linearly polarized radiation at 19.3, 37.0 and 85.5 GHz. In addition it includes a vertical polarized radiation channel at 22.2 GHz. Most applications of the SSMI data have developed multiple regression algorithms from a combination of the above radiances such applications include rain rate algorithms, total precipitable water estimates and ocean surface wind speeds. Halpern *et al.* (1993) have examined this problem in considerable detail and demonstrated the usefulness of this data for the ocean surface wind speed climatology. The following algorithm, based on Halpern *et al.* (1993), was used to deduce the daily surface wind over the Bay of Bengal during the period of the Bangladesh cyclone

$$ws = 147.9 + 1.0969 \times T_B^{19V} - 0.455 \times T_B^{22V} - 1.7600 \times T_B^{37V} + 0.786 \times T_B^{37H}$$

Forecast experiments were run with and without the inclusion of SSMI surface winds over the ocean. The experiment with the SSMI winds exhibited a strong positive impact; a stronger storm resulted from this additional data source. These results are shown in Figures 19 a, b, c and d. Here we provide a summary of results of computations over a 10°

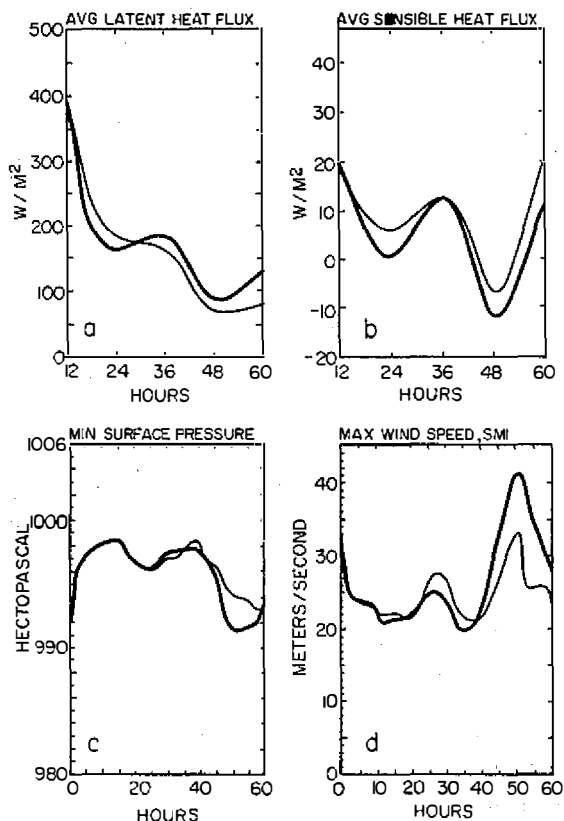


Fig. 19. Averaged values over 10° latitude/longitude squares centered on storm during 60 hour integration of regional model forecasts.

(a) latent heat flux, watts m^{-2} (b) sensible heat flux, watts m^{-2} (c) surface pressure, mb. (d) maximum wind speed, ms^{-1}

Heavy lines: for the experiment with SSMI based surface winds.

Thin lines: for the experiment without SSMI based surface winds.

latitude/longitude square centered over the storms during the 60 hour predictions. In these diagrams the heavy dark curve denotes results for the experiment that included the SSM/I based surface winds. The other curve (thin dark) denotes results for the other experiment where the SSM/I based winds were excluded. The abscissa in all panels denotes hours of forecast for the regional high resolution model. The four panels include results for a) the latent heat flux; b) the sensible heat flux; c) the minimum surface pressure, and d) the maximum surface wind. Overall, we note an enhancement of latent heat flux, a decrease of sensible heat flux, a lowering of surface pressure and an enhancement of the surface winds from the inclusion of the SSM/I based surface wind estimates. It should be noted that these are averages over 10° squares and do not reflect maximum values for the storm. Overall, the storm intensity is an impressive part of the computations.

A summary of the high resolution regional model's forecast, which incorporates the above stated improvements, is shown in Figure 20. Here we illustrate the observed and the predicted tracks on the top left panel. The local orography, which is akin to a side wall boundary for the Bangladesh storm, is shown in the top right panel. The warm SST of the Western Bay (temperature $\simeq 31^\circ\text{C}$) is shown in the center left panel. The wind field at landfall is illustrated in the middle-right panel where the salient feature is the strong winds over the Chittagong area. The rainfall at landfall, shown in the bottom left panel, has maximum amounts of the order of 200 mm day^{-1} over the Chittagong area. The regional model forecasts of the rainfall were somewhat larger than those of the global model (perhaps due to its higher resolution). The rainfall pattern does not include any elongated bounded feature into the central Bay, perhaps a limitation arising from the lateral boundaries at the equatorial end which limits the burst of moisture transport as the cyclone develops. The bottom right panel illustrates a satellite photograph near the time of the landfall. Overall we feel that this is a successful forecast of the landfall of a major tropical cyclone.

8. CONCLUDING REMARKS

In this paper we have presented results of short range prediction experiments from two high resolution models. One of these was a global model at a horizontal resolution of 213 waves triangular truncations (T213) and 15 vertical levels. The other is a regional model which was run at a resolution of roughly 46 km and 15 vertical levels. Both models are fairly comprehensive in their physical parameterization. The specific example addressed here is the Bangladesh cyclone of April 1991 which was a catastrophic storm that resulted in well over 100,000 deaths. This was a supertyphoon strength storm that formed along the ITCZ near 10°N over warm ocean temperatures over the Bay of Bengal. We demonstrated a successful three day forecast of this storm from both the models. The global model's forecast track was very close to the observed track. The success of that forecast came from years of model development in many areas, especially the formulation of physical processes, physical initialization, increase of resolution (see Krishnamurti *et al.*, 1992). The role of sea surface temperatures especially over the western Bay was a crucial element in this prediction experiment. The model sensitivity addressed here came from a series of tests performed by Sukawat (1992) using the FSU regional model at high resolution. The sensitivity experiments were designed by degrading the complete model to study the effects of several surface layer processes. The intensification of the storm over the Bay resulted in a broad cyclonic circulation. A part of that stream traversing over the warm Bay of Bengal SST anomaly contributed a significant enhancement of evaporation. That moist air entered

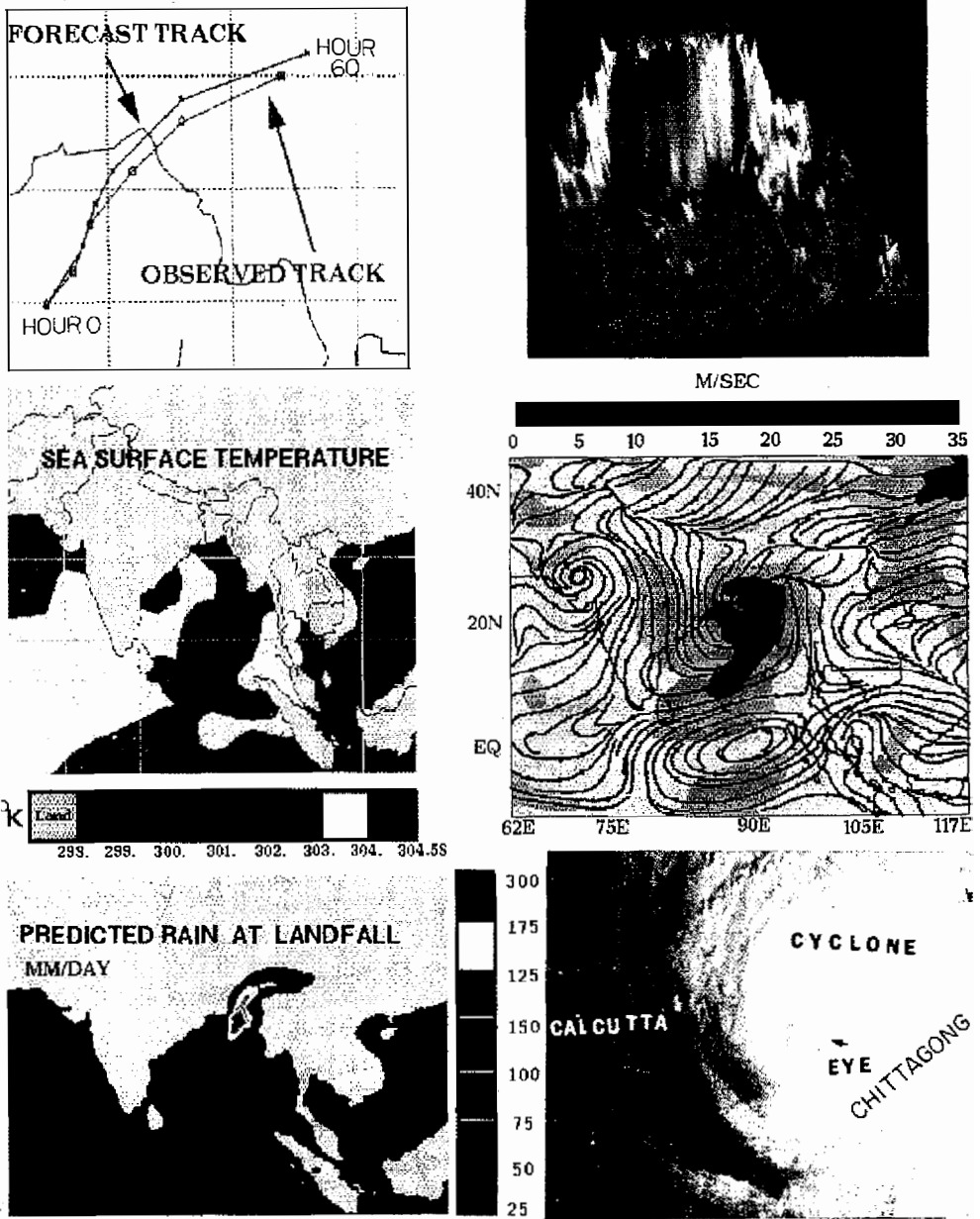


Fig. 20. Top left: observed and predicted tracks; and top right: a 3-D schematic of local orography. Middle left: shows the sea surface temperatures from the JMA data sets; and middle right: shows the predicted 850 mb flow field at landfall. Bottom left: shows the rainfall (mm day^{-1}) rate at landfall and the bottom right shows a visible satellite imagery just prior to landfall.

the storm circulation and helped its further intensification. The storm track and the storm intensity were noted to be quite sensitive to the local orography, especially the Burmese mountains. In its absence the deviations of storms track from the best track position was larger and the storm was more intense (an effect of reduced surface friction).

Other sensitivity studies assess the importance of land surface processes especially that of ground wetness which was brought about by the inclusion of past rain. That appeared to provide some of the best track forecasts on the landfall of the Bangladesh Cyclone. Forecasts made with a simpler ground wetness parameterization had larger track forecast errors.

An important area of data sensitivity came from the inclusion of surface wind speed from the satellite microwave radiometers (the so called DMSP/SSM/I data). Inclusion of this data provided a positive impact on the storm track and storm intensity.

Our studies suggest that the following are some of the important ingredients for the modelling of land falling tropical cyclones

- (a) One needs a high resolution global model with a horizontal resolution of around 50 km (global model at least T170 waves) and 15 vertical levels.
- (b) A sophisticated cumulus parameterization along and near the path of the landfalling storm deserves to be carefully incorporated. Such modelling has led to successful forecasts of several storms such as Typhoon Hope of August 1979, Tropical cyclone over southern India May 1979, Typhoon Colleen 1983, Triple Typhoon over western Pacific September 1987, Hurricanes David and Frederic of 1979 and Andrew of 1992. Further work is needed to explore further improvements of the model parameterization, a scheme capable of resolving rainfall rates of the order of 300 mm/day or higher is necessary.
- (c) Physical initialization and the bogussing of the storm (location, intensity) are extremely important for modelling.
- (d) Areas of other physical parameterization which deserve attention include the detailed estimates of surface fluxes, radiative destabilization of the storm environment and land surface (ground wetness) processes.
- (e) Local orographic details at the model resolution and physical initialization are some of the other areas requiring emphasis.

Acknowledgements This work was supported by NSF grant no. ATM 8812053, ONR grant no. N00014-93-1-0243, NASA grant no. NAG 8-914. Computations for this work were carried out at the NCAR/YMP. NCAR is sponsored by the National Science Foundation.

REFERENCE

- Beljaars, A., and M. Miller, 1990: A note concerning the evaporation from the tropical oceans; sensitivity of the ECMWF model to the transfer coefficient of moisture at low wind speed. ECMWF Research Department Technical Memo 170, ECMWF, Reading, 19pp.
- Businger, J. A., J. C. Wungard, Y. Isumi, and E. F. Bradley, 1971: Flux profile relationship in the atmospheric surface layer. *J. Atmos. Sci.*, **28**, 181-189.

- Dastoor, A., and T. N. Krishnamurti, 1990: The landfall and structure of a tropical cyclone: the sensitivity of model predictions to soil moisture parameterization. *Bound. Layer Meteor.*, **55**, 345-380.
- Frank, Neil L., and S. A. Husain, 1971: The deadliest tropical cyclone in history? *Bull. Am. Meteor. Soc.*, **52**, 438-444.
- Gupta, A., and A. Muthuchami, 1991: El-Niño and tropical storm tracks over Bay of Bengal during post monsoon season. *Mausam*, **42**, 257-260.
- Halpern, D., W. Knauss, O. Brown, and F. Wentz, 1993: An atlas of monthly mean distributions of SSMI surface wind speed, ARGOS buoy drift, AVHRR/2 sea surface temperature, and ECMWF surface wind components during 1990. NASA Jet Propulsion Laboratory publication 93-1, 111pp.
- Harshvardan, and T. G. Corsetti, 1984: Longwave parameterization for the UCLA/GLAS GCM. NASA Tech. Mem. 86072, Goddard Space Flight Center, Greenbelt, MD 20771.
- Kanamitsu, M., 1975: On numerical prediction over a global tropical belt. Report No. 75-1, Dept. of Meteorology, Florida State University, Tallahassee, FL 32306-3034, 1-282.
- Kitade, T., 1983: Nonlinear normal mode initialization with physics: *Mon. Wea. Rev.*, **111**, 2194-2213.
- Krishnamurti, T. N., S. Low-Nam, and R. Pasch, 1983: Cumulus parameterization and rainfall rates II. *Mon. Wea. Rev.*, **111**, 815-828.
- Krishnamurti, T. N., D. K. Oosterhof, and A. V. Mehta, 1988: Air-sea interaction on the time scale of 30 to 50 days. *J. Atmos. Sci.*, **45**, 1304-1322.
- Krishnamurti, T. N., A. Kumar, K. S. Yap, A. P. Dastoor, N. Davidson, and J. Sheng, 1990: Performance of a High-resolution mesoscale tropical prediction model. *Adv. Geophys.*, **32**, 133-281.
- Krishnamurti, T. N., J. Xue, H. S. Bedi, K. Ingles, and D. Oosterhof, 1991: Physical initialization for numerical weather prediction over the tropics. *Tellus*, **43**, 53-81.
- Krishnamurti, T. N., K. S. Yap, and D. Oosterhof, 1991: Sensitivity of tropical storm forecast to radiative destabilization. *Mon. Wea. Rev.*, **119**, 2176-2205.
- Krishnamurti T. N., D. K. Oosterhof, and H. S. Bedi, 1992: Hurricane Forecasts in the FSU Models. *Adv. Atmos. Sci.*, **10**, 121-131.
- Lacis, A. A., and J. E. Hansen, 1974: A parameterization for the absorption of solar radiation in the earth's atmosphere. *J. Atmos. Sci.*, **31**, 1889-1909.
- Louis, J. F., 1981: A parametric model of vertical eddy fluxes in the atmosphere. *Bound. Layer Meteor.*, **17**, 187-202.
- Machenhauer, B., and E. Rasmussen, 1972: On the integration of the spectral hydrodynamical equation by a transform method. Report No. 3, Institut for Teoretisk Meteorologi, Kobenhavns Universitet, Denmark, 44pp.
- Pasch, R. J., 1983: On the onset of the planetary scale monsoon. Ph. D. Dissertation, Dept. of Meteorology, Florida State University, Tallahassee, FL 32306-3034, 220pp.
- Sukawat, D., 1992: Sensitivity of a Bangladesh cyclone to surface parameters. Ph. D. Dissertation, Dept. of Meteorology, Florida State University, Tallahassee, FL 32306-3034, 141pp.

- Thu, T. V., and T. N. Krishnamurti, 1992: Vortex initialization for typhoon track prediction. *Meteor. Atmos. Phys.*, **47**, 117-126.
- Tiedke, M., 1984: The sensitivity of the time-mean large-scale flow to cumulus convection in the ECMWF, Nov. 28-Dec. 1, 1983, 297-316.
- Wallace, J. M., 1971: Spectral studies of tropospheric wave disturbances in the tropical western Pacific. *Rev. Geophys. Space Phys.*, **9**, 557-612.
- Wallace, J. M., S. Tibaldi, and A. J. Simmons, 1983: Reduction of systematic forecast errors in the ECMWF model through the introduction of envelope orography. *Quart. J. Roy. Meteor. Soc.*, **109**, 683-718.